ChemMedChem

Chemistry Europe
European Chemical Societies Publishing

Accepted Article

Title: Theranostics through the synergistic cooperation of heterometallic complexes

Authors: M. Concepción Gimeno, Marta Redrado, Vanesa Fernández-Moreira, and M. Concepción Gimeno

To be cited as: *ChemMedChem* 10.1002/cmdc.202000833

Link to VoR: https://doi.org/10.1002/cmdc.202000833

WILEY-VCH

10.1002/cmdc.202000833

WILEY-VCH

Theranostics through the synergistic cooperation of heterometallic complexes

Marta Redrado[a], Vanesa Fernández-Moreira*[a] and M. Concepción Gimeno*[a]

Dedication ((optional))

[a] M. Redrado, Dr. V. Fernández-Moreira, Prof. Dr. M. C. Gimeno.
Departamento de Química Inorgánica,
Instituto de Síntesis Química y Catálisis Homogénea (ISQCH), CSIC-Universidad de Zaragoza
Pedro Cerbuna, 12, *50009 Zaragoza, Spain*.
E-mail: vanesa@unizar.es and gimeno@unizar.es

Abstract: Heterometallic drugs are emerging as a great alternative to conventional metallodrugs. The careful selection of the different metallic fragment makes it possible to enhance, not only the therapeutic potential by a synergy effect, but also the incorporation of key features like traceability. Drugs that integrate traceability and therapy in one system are known as theranostic agents. Among cancer research, theranostic agents are becoming increasingly important. They deliver crucial information regarding their biological interplay that can be ultimately used for the optimization process. The well established therapeutic potential of Pt^{II}, Ru^{II} and Au^{I} based drugs, combined with the outstanding optical properties of d^6 transition metal complexes grant the delivery of traceable metallodrugs. These species can be easily fine-tuned through modifications of their respective ligands to deliver a new generation of drugs.

Figure 1. Example of metallodrugs approved by the FDA and at the stage of clinical trials.

Introduction

Barnet Rosenberg discovered that cisplatin possessed a potent chemotherapeutic action in 1965,[1] and later in 1978, cisplatin was approved by the FDA as treatment for testicular and advanced ovarian and bladder cancer. Since then, research into the mode of action of cisplatin and second generation of platinum based drugs (oxaliplatin and carboplatin) have encouraged many investigations, Figure 1.[2] Great efforts have been devoted to improve their efficiency while decreasing their secondary effects, that basically arise from their indiscriminate attack on all rapidly dividing cells.[3] Despite that, it is well accepted that cisplatin opened the door to study other transition metal complexes for the treatment of cancer.[4] Nowadays, ruthenium and gold complexes together with platinum-based drugs appear to be leading the research into the development of novel metallodrugs.[5] In fact, complexes derived from those metals such as NAMI-A, KP1019 and Auranofin reached different clinical trial phases for diverse cancer diseases (Figure 1). In many cases, the lack of other effective treatments forces the extensive use of platinum drugs leading to drug resistance. Therefore, it is expected that the introduction of additional metallodrugs as standard treatments, would help to overcome such increase of the platinum drug resistance and to deal effectively with a wider range of cancers.

One of the major drawbacks in the development of advanced medicines is the lack of knowledge of their biological interplay. Gaining such information is crucial for the optimization of the drugs that will eventually endow specificity and effectiveness improving considerably the society wellbeing. Thus, the concept of theranostic agents has emerged as a revolution among the medical community. Theranosis involves diagnostic and therapeutic functions in one combined system, allowing diagnosis, therapy, and monitoring of therapeutic response at the same time, Figure 2.[6] For the diagnostic and monitoring function it is required the use of noninvasive imaging modalities. Among them, there are different techniques such as Position Emission Tomography (PET), Single Photon Emission Computer Tomography (SPECT), Computed Tomography (CT), Magnetic Resonance Imaging (MRI) or fluorescence microscopy that can be used. However, the different strengths and weaknesses displayed by each modality in terms of tissue penetration, resolution or applicability, make sometimes difficult to select one.[7] Thus, from our point of view, after considering the high cost of some of the techniques (MRI, CT, PET and SPECT) together with the necessity of using radionuclides or isotopes (MRI, PET and SPECT) in others, fluorescence microscopy stands out a good alternative for drug visualization.

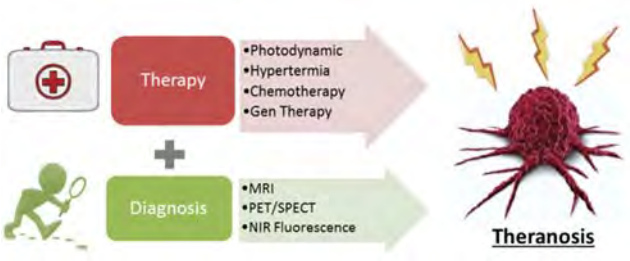

Figure 2. Pictogram describing the different possibility for theranostic agents.

Fluorescence microscopy imaging is a powerful technique that can be performed on live cells.[8] It has various advantages including sensitivity, real-time visualization or non-ionization safety, which make the delivery of novel optical probes very appealing. The sub-micro molar detection of fluorophores and the possibility of collecting multiple wavelengths simultaneously allow the use of specific organelle stains that considerably facilitates the assessment of the biodistribution. However, an obvious limitation would be having optical probes that emit within the detectable wavelength window, i.e. in the UV - NIR range, the latter being preferable because of the greater depth tissue penetration. NIR-II organic fluorophores have emerged as one of the alternatives to circumvent such limitation. These fluorophores emit at the second near- IR region between 1000 and 1700 nm, offering deep light penetration and low auto-fluorescence.[9] Some examples of those combined with platinum based metallacycles have provided very promising metalo-based theranostic platforms for efficient imaging and therapy.[10] Alternatively, metal-based optical probes are also ideal candidates as most of them displayed a phosphorescent emission. In particular, complexes derived from d^6 metal complexes have been recently used as optical probes for cell imaging.[11] Their emission properties, easily tunable by simple functionalization of the coordinated ligands, afford a wide range of possibilities ranging from blue to red emitters.[12] Moreover, their excited state lifetimes, much longer to those of endogenous fluorophores (0.1-7 ns)[13] facilitate the use of time-gated techniques that eliminate autofluorescence of the sample and renders images with greater signal-to-noise ratio. [14]

Taking into account the advantages displayed by metallic complexes in cellular imaging, and the importance of cellular tracking for the development of novel and more effective metallodrugs, the idea of combining a metallic bioprobe with a luminescent complex to function as tracking tag is very appealing. By this means, the concept of heterometallic theranostic agents arises, and every day is gathering more supporters among the research community. Although in early 2018 our research group published a concept article on heterobimetallic probes as theranostic agents,[15] the increasing amount of research published since them, makes this subject worthy of an update. Therefore, in this concept article, we gather the reported examples dealing with heterometallic complexes that have shown promising properties as theranostic agents. We will focus on species combining luminescent d^6 metal complexes with potential bioactive metallodrugs derived from Pt^{II}, Ru^{II} and Au^{I}, as complexes derived from those metals have already shown their great projection in therapy. Finally, we will highlight the strengths of heterometallic theranostic probes and we will discuss the future challenges that need to be addressed in order to eventually deliver a heterobimetallic theranostic probe into clinical trials.

Heterometallic metallodrugs

Among the published reports dealing with the search of novel metallodrugs, can be found examples of heterometallic complexes based on the hypothesis that combination of two cytotoxic metals may enhance the cytotoxic potential as well as overcoming drug resistance.[16] In fact, in most of the cases this idea is validated, and polynuclear complexes turned to be potent inhibitors off cancer cells with a significant improvement compared with their mononuclear parent species.[17] Thus, Figure 3 illustrates some examples combining fragments derived from Ru^{II}, Pt^{II}, Au^{I}, Ti^{IV}, Cu^{II}, Ag^{I}, Ir^{III} or Fe^{II}, some of them with analogous chemical structures to that of RAPTA-T, cisplatin, auranofin, titanocene of ferrocene, have been combined to deliver species with enriched cytotoxicity towards different lines of cancer cells (**1**-**7**).[18] Among them, there are specific examples that bring together bioactive species with well-known emissive complexes, examples **A** and **B** in Figure 3.

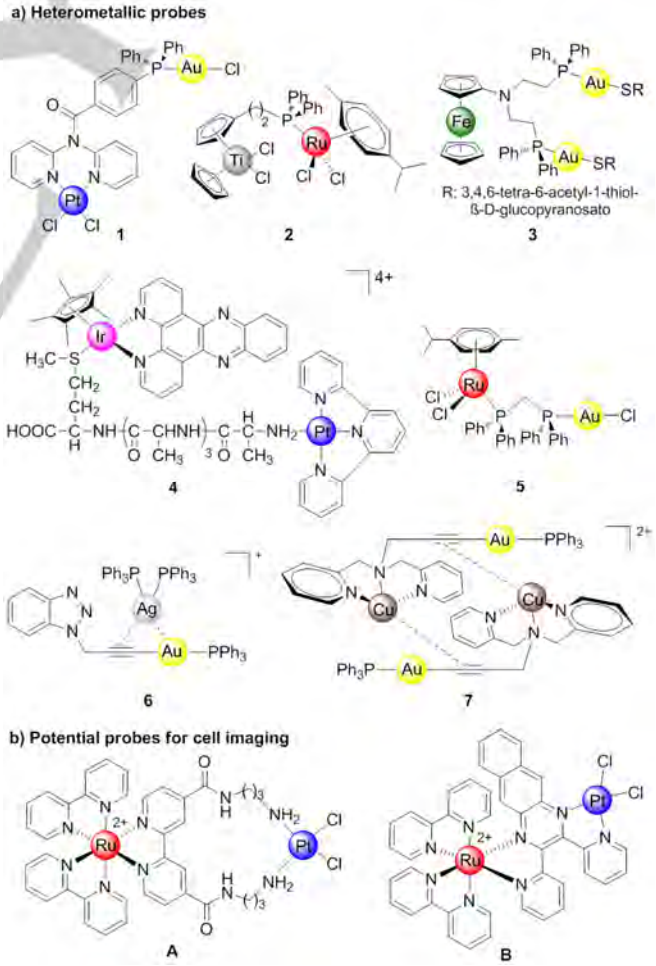

Figure 3. Heterometallic bioprobes including specific examples with potential application in bioimaging.

However, even though they have demonstrated to be cytotoxic and to interact with a specific biological target, no studies dealing with their cell biodistribution were performed.[19] Therefore, there is no assurance that the molecule reaches the assumed target in a cellular environment.

As previously observed optical theranostic probes can be easily tracked inside cells by fluorescence microscopy. Thus, this visualization technique in combination with a theranostic agent make possible to demonstrate that the probes are able to reach the specific organelle or biological target where the therapeutic action is undertaken. Without such information, it is very difficult to ensure that the probe will have a specific action mechanism. There are probes that due to their chemical structure, for instance, the presence of planar aromatic ligands, or specific metal centers such as Au^{I}, are known to selectively interact with DNA or with enzymes like thioredoxin reductase (TrxR) respectively.[20,21] However, their biological interplay can be very different if the probes are not able to reach their assumed biological targets. Therefore, the approach towards the development of a new drug when it comes to deliver theranostic probes is completely different. The interaction with the biological target is studied after knowing the information of the inner cellular biodistribution by visualization techniques.

Heterometallic $Re^{I}Au^{I}$ bioprobes for theranostic applications

The first heterometallic d^6-d^{10} emissive probes designed for tracking and therapy applications was developed by our research group in 2014.[22] Thus, a series of luminescent $Re^{I}Au^{I}$ derivatives were described by the combination of a well-known emissive Re^{I} core, *fac*-{$Re(bipy)(CO)_3$}, and a potential bioactive Au^{I} species of the type C-Au-P, Figure 4, complexes **8**-**11**. Both fragments were connected through an alkynyl pyridine/imidazole derivative by a stepwise synthetic procedure. The excellent photophysical properties of the Re^{I} fragment allowed tracking the biodistribution of the probes in lung cancer A549 cells. Moreover, the analysis of the cytotoxic activity of each monometallic fragment disclosed IC_{50} values over 120 μM indicating that the therapeutic potential was exclusively due to the Au^{I} fragment, being the role of the Re^{I} fragment relegated to visualization purposes, see table b in Figure 4. Fluorescence microscopy showed a different biodistribution driven by the loading concentration of the probes. Thus, localization of the probes shifted from the cytoplasm, possibly in the mitochondria, to the nucleus and nucleolus upon increasing the loading concentration over the IC_{50}.[22]

Since them related examples have been published combining $Re^{I}Au^{I}$ metal centers in order to optimize the metallic combination. Analogous heterometallic probes **12**-**17**, preserving the emissive Re^{I} core and exploring diverse Au^{I} coordination sphere (P-Au-P, or P-Au-Cl) were described.[23] However, their antiproliferative potential towards A549 cells were lower than in the previous examples **8**-**11**. The overall cytotoxicity resulted to follow the trend (C-Au-P) > (P-Au-P) > (P-Au-Cl) for the Au^{I} fragment. A similar biodistribution pattern was observed for **16** and **17**, with a non-uniform cytoplasmic distribution as well as nuclear permeation, and further studies revealed DNA interaction and passive diffusion as the entrance pathway.[23]

Additional heterometallic probes, where the typical Re^{I} luminescent core was this time modified to *fac*-{$Re(NHC)(CO)_3$}, were described (species **18**-**20** in Figure 4a).[24] These species had a blue shifted emission (λ_{em} < 500 nm) to that published so far with the diimine-Re^{I} system, leading to poorer systems for bioimaging applications. In fact, only complexes **18** and **19** could be followed by fluorescence microscopy. Their antiproliferative potential was similar to that of species **8** to **11**, indicating again the high dependence on the nature of the Au^{I} coordination sphere to reveal the cytotoxicity. Moreover, these species showed an increment of the cytotoxicity upon irradiation, which is encouraging to proceed towards photodynamic therapy applications, see footnote on the table of Figure 4.[24]

Alternative $Re^{I}Au^{I}$ probes, where the bioactive fragment was introduced within the emissive Re^{I} core, were also reported, species **21**-**25** in Figure 4.[25] This is a new approach to those described so far. Any changes on the bioactive fragment could be monitored by fluorescence techniques, giving the information of the precise moment of interaction with the biological target. In fact, we demonstrated that monometallic Re^{I} and heterometallic $Re^{I}Au^{I}$ species as well as a substitution of gold ancillary ligand in $Re^{I}Au^{I}$ lead to modifications on the emission maxima. Overall it was revealed that these species had selectivity and higher cytotoxicity towards cervix cancer HeLa cells than in the case of A549 cells at long incubation times (72h). Fluorescence microscopy showed that the complexes were biodistributed differently in both cell lines, being this the trigger for the different effect. Thus, whereas complexes interact with the cellular membrane of HeLa cells, they were randomly distributed in A549 cells, Figure 4c, complex **22**.[25]

In summary, the bimetallic $Re^{I}Au^{I}$ library, developed entirely by our research group, have outlined several guidelines to be able to deliver optimized optical theranostic agents containing these metal centers. The low biological media solubility displayed by some species can be overcome by either substitution of the gold ancillary ligand or removing the chloride of the rhenium core for a neutral donor ligand. Typically, substitution of the halide ligand in the Re(I) core for a N-donor ligand renders greater solubility as the character of the Re^{I} core changes from neutral to cationic. Moreover, extending the aromaticity or electron movement along the chelated (N^N) ligand improves the light depth penetration of the probe. Moreover, a careful selection of the gold ancillary ligand renders modulation of the antiproliferative activity of the probe.

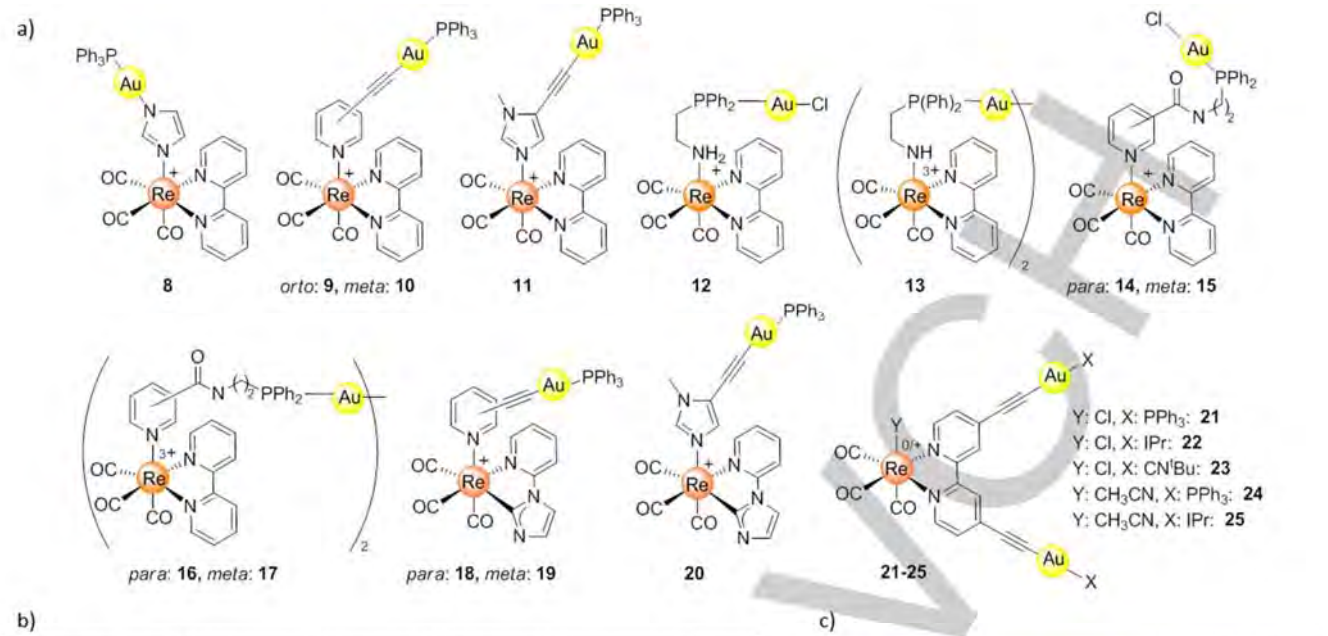

b)

Complex $Re^{I}Au^{I}$	A549 24h	A549 24h[b]	A549 72h	HeLa 24h	HeLa 72h
8[a]	19 ± 9.7	-	-	-	-
9[a]	9.5 ± 1.0	-	-	-	-
10[a]	9.7 ± 1.1	-	-	-	-
11[a]	4.4 ± 0.5	-	-	-	-
12	64.69 ± 3.3	-	-	-	-
13	35.82 ± 1.82	-	-	-	-
14	75.25 ± 10.6	-	-	-	-
15	67.80 ± 4.11	-	-	-	-
16	42.44 ± 1.03	-	-	-	-
17	36.09 ± 16.9	-	-	-	-
18	10.82 ± 1.63	2.66 ± 0.57	-	-	-
19	12.28 ± 1.19	4.48 ± 1.71	-	-	-
20	12.65 ± 2.10	9.97 ± 3.04	-	-	-
21	> 50	-	> 25	> 25	6.46 ± 0.35
22	> 50	-	> 25	> 25	> 25
23	> 50	-	> 25	> 25	10.79 ± 0.48
24	> 25	-	17.52 ± 1.4	18.8 ± 1.15	2.35 ± 0.06
25	> 25	-	> 25	> 25	16.4 ± 2.80

[a] IC_{50} monometallic Re(I) species derived from **8**, **9**, **10** and **11** > 120 μM. [b] IC_{50} (A549, 24h, λ_{ex}: 405 nm for 10 min)

c)

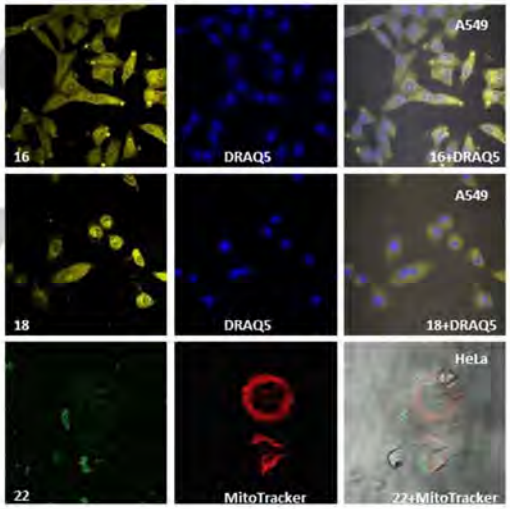

Figure 4. a) Reported examples of Re(I)/Au(I) theranostic agents. b) IC_{50} data of complexes **8**-**25** in different tumor cellular lines and different conditions. c) Biodistribution profiles of **16**, **18** and **22** in AA549 cells. [19] - Reproduced by permission of The Royal Society of Chemistry. Adapted with permission from ref [20]. Copyright (2017), ref [21]. Copyright (2018), ref [22]. Copyright (2020), American Chemical Society.

Heterometallic Ru^{II}-based bioprobes for theranostic applications

In 2015, the first examples dealing a heterometallic emissive Ru^{II} and a bioactive Au^{I} species was described by the hand of Hemmert and Gornitzka.[26] They funtionalized the typical emissive $[Ru(bipy)_2(N^N)]^{2+}$ core, where N^N represent a diimine ligand, with an imidazole derivative that later was used as linker for the Au^{I} fragment, Figure 5. Thus, the correspondent gold-NHC complex obtained was expected to deliver high cytotoxicity as many other gold-NHC compounds had demonstrated.[27] However, even though complexes **26**-**28** presented certain bioactivity, they did not improve that given by Sorafenib, a commercial available drug used as reference compound. Despite of that, observation of luminescent properties revealed that the presence of Au^{I} fragment do not interfere with emission of the Ru^{II} fragment but increased its quantum yield, making them very appealing for bioimaging applications. Complex **27** localized in the cytoplasm, mainly in the peripheral area of the nuclei of liver cancer cells Hep3B, Figure 5. Changes in the emission maxima wavelength observed in time dependent fluorescence microscopy experiments suggested that the gold fragment was being released within the cell over time.

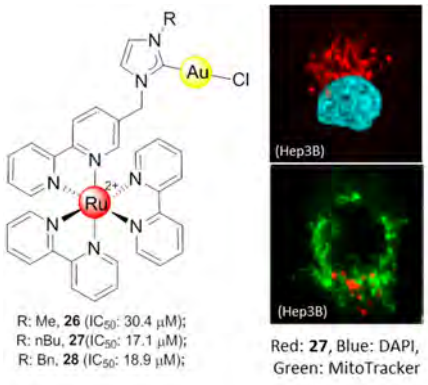

Figure 5. IC_{50} data of complexes **26**-**28** in human hepatocellular carcinoma cell (Hep3B). Cellular biodistribution of **27**. Adapted with permission from ref [23]. Copyright (2015) American Chemical Society

Thereafter similar heterobimetallic probes were reported by Casini, Bodio and coworkers.[28] This time the gold coordination sphere was modified to have a similar structure to that of auranofin in order to increase as much as possible its therapeutic potential. Thus, the bifunctional diimine ligand used as linker between both metallic fragments has a phosphorus donor atom able to coordinate the Au^{I} center. Moreover, the gold coordination sphere was completed with a thioglucose, Figure 6. Additional modifications on the optical Ru^{II} properties were made with the introduction of a 2,2-dipyridyl amine instead of the previous bipyridine ligand. As expected, $Ru^{II}Au^{I}$ complexes containing the thioglucose (**31**, **32**) instead of the chloride (**29**, **30**) had greater cytotoxicity, corroborating the strong influence of the gold ancillary ligands on the therapeutic potential. All of them are emissive, **29** and **31** being the stronger emitters. Moreover, they permeated the cell via an active transport mechanism. Both thioglucose derivatives showed different cellular biodistribution. Whereas **31** accumulated in the cytoplasm, **32** was located in the nucleus and organelles therein, outlining that, not only the bioactive Au^{I} fragment participates on the biodistribution, but also the luminescent Ru^{II} core is implicated.

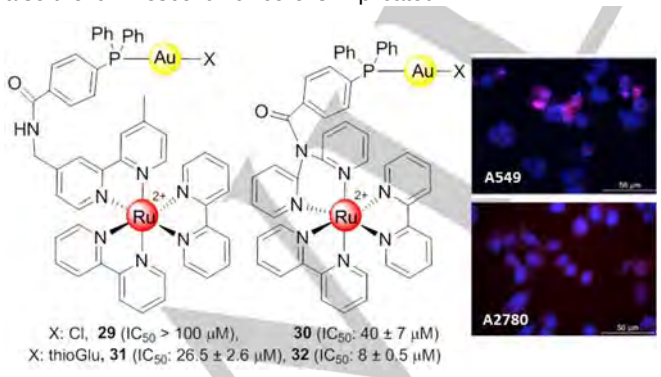

Figure 6. IC_{50} data of complexes **29**-**32** lung cancer cells (A549). Cellular biodistribution **31** (upper picture) and **32** (lower picture). Complexes in pink, DAPI (nuclear dye) in blue. Adapted with permission from ref [25]. Copyright (2016) American Chemical Society

Alternatively to the $Ru^{II}Au^{I}$ combination, an example including a Pt^{II} based fragment with a similar structure to that of cisplatin has been reported. Thus, Thomas, Smythe and coworkers described a $Ru^{II}Pt^{II}$ complex that can be used as a DNA light switch drug, Figure 7a.[29] The authors rely on both, the well-known DNA interaction of cisplatin different to that of bisimine Ru^{II} cores, and the luminescence enhancement observed for latter in presence of DNA, Figure 7b. Eventually, it was found that the heterobimetallic complex **33** had lower cytotoxicity than cisplatin in ovarian cancer cell lines A2780, but no significant change was seen towards platinum resistant A2780CIS, suggesting that the platinum resistance was not governed by the DNA interaction mode. Optical properties of the complex allowed to visualize structural changes on the interaction mode of the complex with DNA, monitoring the switch from intercalation to groove binding as well as investigating the cell death timing. Thus, live-cell fluorescence microscopy suggested a fast cell death mechanism though oncosis, characterized by loss of cytoplasmic volume control among other features, see Figure 7c.

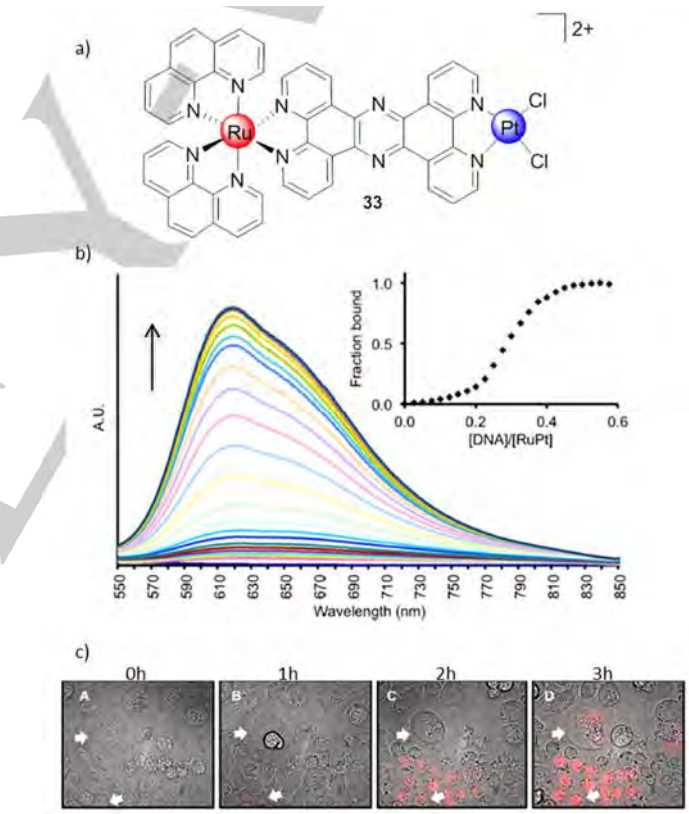

Figura 7. a) Depiction of **33**. b) Increase in luminescence of **33** on addition of calf thymus DNA (λex = 450 nm). Inset: Derived binding curve from these data. c) Time dependent cellular uptake of **33** into A2780. Images show luminescence arising from MLCT superimposed on phase contrast micrographs. Arrows indicate examples of oncotic cell swelling. Adapted with permission from ref [26]. Copyright (2019) American Chemical Society

Heterometallic Ir^{III}- based bioprobes for theranostic applications

Ir^{III} complexes bearing cyclometallated ligands exhibit well-known optical properties, with capability for being used in

cellular imaging,[30] as well as, a great stability in biological media. For this reason, they are excellent candidates to be used as emissive tags of therapeutic drugs. In addition, many cyclometallated Ir^{III} species have shown to be active as photosensitizers in photodynamic therapy,[31] opening the door to the design of multimodal species. Moreover, cyclometallated Ir^{III} compounds of the type $[Ir(N^C)_2(N^N)]^{0/+}$, where N^C represent an orthometallated ligand, display general features such as an easy synthesis and air and moisture stability, reinforcing their medicinal potential as part of a heterometallic theranostic agent.

In 2014, a hetero-binuclear $Ir^{III}Ru^{II}$ complex, **34**, was developed by Kim, Patra and co-workers, Figure 8.[32] The idea behind their design was to gain insight on drugs that trigger autophagy, as these drugs can kill cells resistant to apoptosis. For that, the authors relayed on synergistic interaction of the multimetallic framework combined with polypyridyl ligands, which are known to enhance the cellular uptake.[33] In fact, complex **34** was highly cytotoxic towards cisplatin resistance MCF7 cancer cells as well as in other cell types. The formation of acidic vacuoles in MCF7 cells in presence of **34** was key for suggesting its capacity to induce autophagy, Figure 8. Therefore, this was the first example of trackable heterodinuclear $Ir^{III}Ru^{II}$ complex with capacity to produce autophagy.

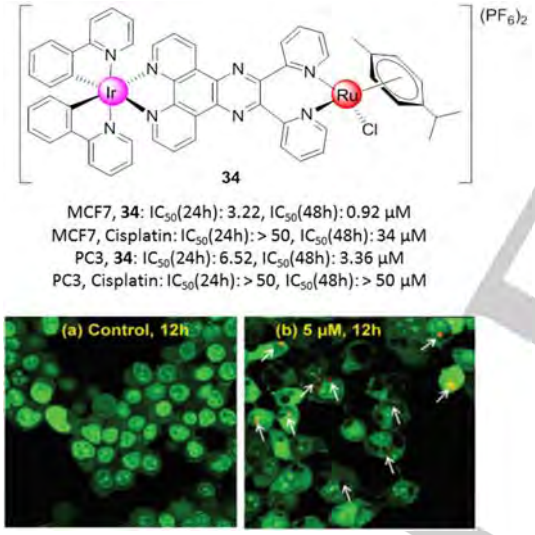

Figure 8. Chemical structure of **34** and related cytotoxicity in MCF7 and PC3 cell lines**.** Overlapped fluorescence microscopy images (a) acridine orange stained and (b) acridine orange stained and complex **34**.

Recently, our research group in collaboration with that of Metzler-Nolte also contributed to the development of heterometallic Ir^{III}-based bioprobes for theranostic applications. We synthetized diverse $Ir^{III}Au^{I}$ peptide bioconjugates, complexes **35** and **36**, Figure 9, with the idea that the peptide will assist to improve water solubility and facilities cell recognition of the probe.[34] The introduction of the gold fragment was achieved via coordination through different groups (alkynyl or sulfur) present in the peptides. We demonstrated a lysosomal accumulation for all the complexes. However, only the species **36**, which contains a cysteine, displays cytotoxic activity towards A459 cell line. Interestingly, this behavior suggested that the strength of the Au-ligand bond could play a crucial role. While Au-S(cysteine) bond was more readily cleaved in a biological environment, the Au-C(triazole) bond was presumably more stable, and thus gold fragment might remain linked to the peptide, which is trapped in the lysosome, preventing cytotoxicity [35].

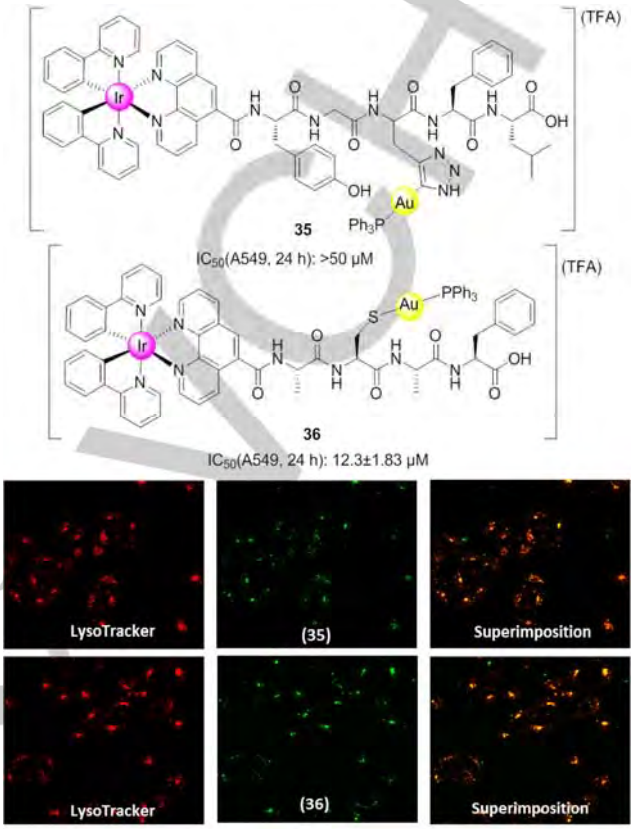

Figure 9. Chemical structures of compounds **35** and **36** and fluorescence microscopy images of a colocalization experiment of **35** and **36** with LysoTracker-red in A549 cells.

Unconventional heterometallic based bioprobes

Apart from the heterometallic complexes described so far, containing two metallic fragments well differentiated for either bioimaging or therapy, there are analogous complexes where no specific therapy based fragment is present. Instead, a completely different metallic fragment to the conventional cisplatin, auranofin or RAPTA-T is included. Therefore, in principle, it is not possible to assign the bioactivity to one of the metal fragments itself, unless one of them clearly displays cytotoxicity upon irradiation. For the other bimetallic species, the combination of both fragments and the subsequent synergy effect are governing their therapeutic effect. Several examples can be found for different bimetallic species, $Ir^{III}Ru^{I}$ and $Re^{I}Ru^{II}$. Thus, in 2014, two research groups, one of them headed by X. Peng and the other one by J. A. Thomas, reported simultaneously the first examples of these unconventional heterometallic based bioprobes.[36,37] Both examples dealt with heterodinuclear $Ir^{III}Ru^{II}$ complexes. Surprisingly, the studies demonstrated significant DNA/rRNA–binding affinities for the different probes. In one hand, Peng and co-workers,[36] developed a heterobimetallic complex, **37**, which

showed a dual-emissive response in the green and orange region (523 nm and 615 nm). Colocalization experiments confirmed the nucleolar localization of the complex, as well as, suggested a high binding affinity of the complex towards RNA, see Figure 10.

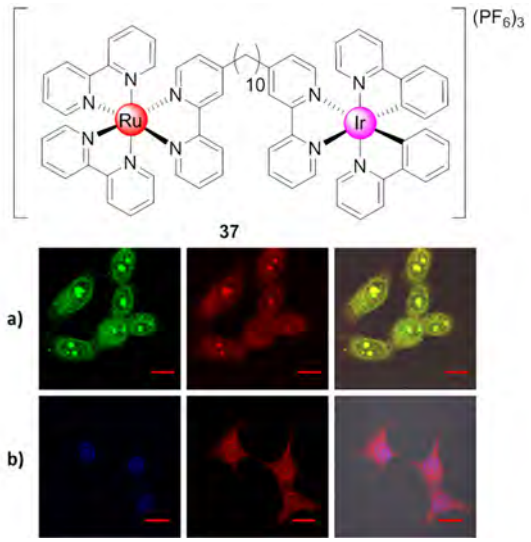

Figure 10. Chemical structure of **37** a) Co-staining of **37** with SYTO RNA-Select dye. Left: RNA-Select dye (green channel); Middle: **37** (red channel); Right: merged image. b) Colocalization of **37** and Hochest33258. Left, Hochest33258 (blue channel); Middle, **37** (red channel); Right, merged image. Scale bar: 20 μm.

On the other hand, the group headed by J. A. Thomas prepared two new luminescent dinuclear $Ir^{III}Ru^{II}$ complexes, **38** and **39**.[37] These compounds displayed good water solubility and affinity for DNA-binding. Additionally, cellular studies demonstrated nuclear uptake, which was enhanced for the fluorinated-derivative **39**, targeting the nucleus more rapidly than the non-fluorinated, complex **38**.

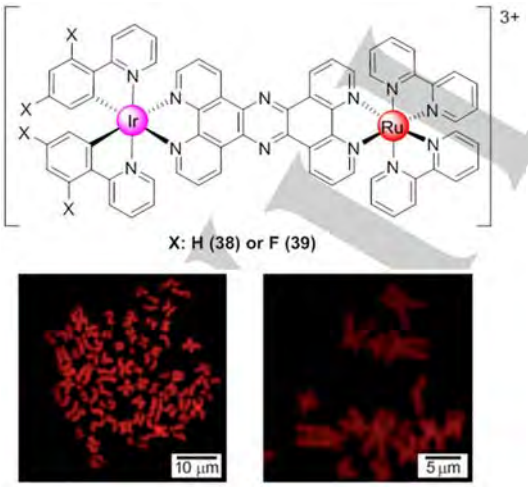

Figure 11. Chemical structure of complexes **38** and **39** and isolated HeLa chromosomes stained with **38**, in metaphase spreads.

In a similar manner, Chao et al.[38] synthetized an additional $Ir^{III}Ru^{I}$ complex, this time as a bifunctional agent for photoactivated chemotherapy and photodynamic therapy, Figure 12. The idea was to use the Ir^{III} fragment to target mitochondria meanwhile using the Ru^{II} species to induce the mtDNA damage. In fact, complex **40**, exhibited antitumor activity towards cisplatin-resistant cancer cells and specifically accumulates in mitochondria. Furthermore, complex **40** could generate $^1O_2$ only under step-wise irradiation, after irradiating at 450 nm and then at 405 nm, Figure 12. Additionally, the heterobimetallic complex was able to induce mitochondrial dysfunction, leading to the loss of mitochondrial membrane potential (MMP), promoting an

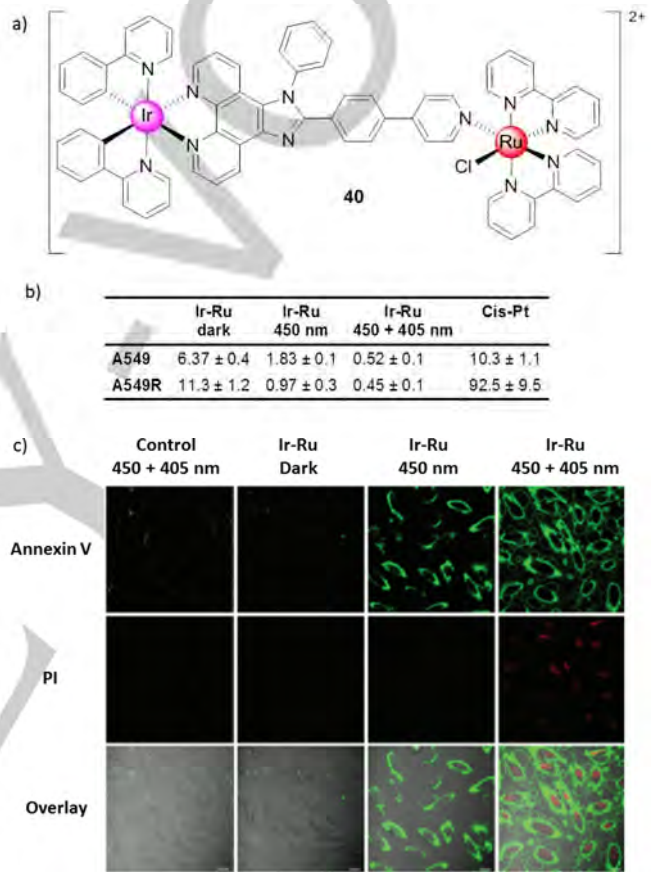

apoptotic cell-death pathway.

Figure 12. a) Chemical structure of complex **40**. b) Cytotoxicity in lung cancer cells A549, in cisplatin resistant lung cancer cells A549R. c) study of cell apoptosis by Annexin V-FITC/PI co-staining assay in A549R cells after complex **40** treatment with or without irradiation.

Alternative to the development of $Ir^{III}Ru^{II}$ probes, J. A. Thomas and C. Smythe also pioneered the work on the bimetallic $Re^{I}Ru^{II}$ complexes, where the ruthenium fragment differs from that of the typical RAPTA-T derivative, used so far in the conventional heterobimetallic theranostic examples containing a Ru^{II} fragment for therapy. The first work entailed a metallomacrocycle, species containing two $[Ru(bipy)_2(N^N)]^{2+}$ units, where the N^N was a quaterpyridine derivative used as bridge ligand between Re^{I} and Ru^{II} metallic centers, Figure 13.[39] Complex **41** showed different cell localization depending on the experimental method used, *i.e.* fixed or life cell studies. Thus, **41** mainly localized in the nuclear membrane and the endoplasmatic reticulum (ER) of fixed MCF7 cells. However, in live cell imaging studies, time-dependent

localization and morphological changes were observed. At the beginning of the experiment, only plasma membrane was stained. Then, nuclear and nucleolar localization was observed. Eventually a general nuclear membrane and other organelle membranes as well as ER were stained followed by a gross cell swelling that leaded to cell death. Alternatively, the cells incubated with **41** in the dark kept normal morphology indicating that the $Ru^{II}Re^{I}$ complex functioned as a potent photosensitizer though ROS generation.

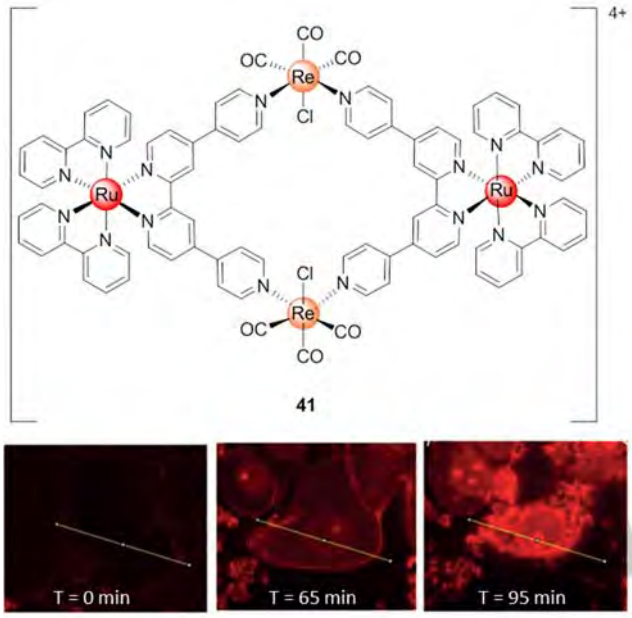

Figure 13. Chemical structure of **41** and time dependent fluorescence microscopy images of **41** incubated with live MCF7 cells.

Recently, the same research group also developed novel $Re^{I}Ru^{II}$ complexes linked by simple dipyridyl alkane ligands.[40] This time the typical tris-bisimine Ru^{II} structure was substituted for a tripodal tris(1pyrazolyl)methane (tpm), a dipyrido[3,2-a:2',3'-c]phenazine (dppz) and a dipyridyl alkane ligand that was used as connector between the Ru^{II} and Re^{I} fragments, see Figure 14. The nature of the dipyridyl linkers affects the biodistribution as well as photostability. Thus, **42** showed low photostability and localized in the nucleus of ovarian cancer cell line A2780, whereas **43** cells has negligible photobleaching and its localization is concentration dependent, going from cytosol to the nucleus upon increasing the loading. Regarding the cytotoxicity, only complex **43** presented similar antiproliferative activity to that of cisplatin. Both complexes bind to DNA with similar affinities, however, it seems clear that the nature of the linkers is affecting their final bioactivity potential.

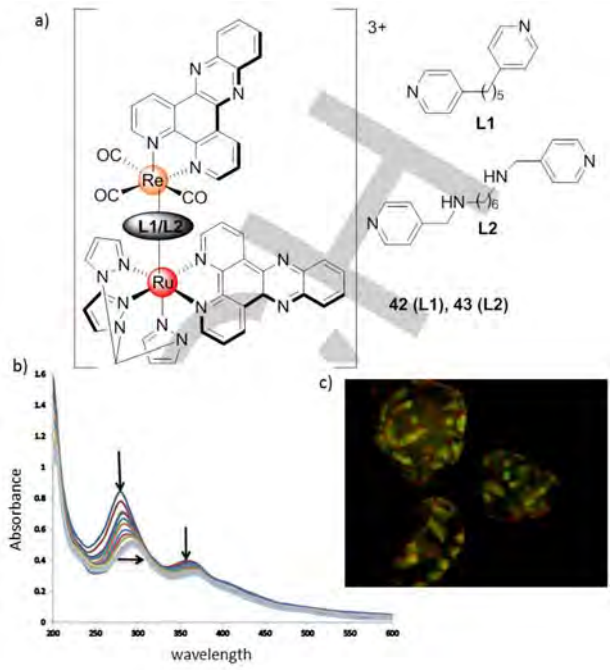

Figure 14. a) Chemical structure of **42** and **43**. b) UV-visible study of DNA interaction with **43**. c) Image of a colocalization experiment of **43** with H33342, a nuclear commercial available dye. Adapted with permission from ref [36]. Copyright (2020) American Chemical Society.

STRENGTHS, FUTURE CHALLENGES OF HETEROMETALLIC THERANOSTIC PROBES AND CONCUSIONS

The lack of understanding of the mechanism of action of a drug is one of the main handicaps for not being able to succeed in the delivery of effective drugs that can pass to clinical trials. Therefore, tracking the drug at every stage gives crucial information that can be used for a better drug design. Opting for a d^6 metallic fragment over an organic chromophore for the imaging process offers clear advantages on the quality and resolution of the images, overcoming typical problems of organic chromophores specially those related with photostability. Consequently, the enhanced relative photostability of transition metal complexes enables their application in long-term observation as well as in dynamic monitoring of living biological systems. Even though sometimes the synthetic pathway for a bimetallic theranostic agent might seem more complicated than that for organic-based derivatives, there are three main synthetic strategies that can be used to easy their preparation: a) synthesis separately of each metallic fragment followed by coupling step, b) design of a bifunctional chelate ligand to selectively bind each metallic fragment and c) a stepwise synthesis.

On the therapeutic aspect, metals are endowed with unique properties not found in conventional carbon-based drugs. Therefore, exploration of metal -based drugs should lead to new therapies able to reduce side effect, increase the spectrum activity and, more importantly, overcoming drug resistance already seen by conventional drugs. The examples reported herein, heterometallic theranostic optical probes, are attracting a growing interest especially in the last years. However, research on the subject is still at the beginning of the pathway, and the

developed systems, although being very promising, are still far from the clinical stage. Finding a therapeutic synergy effect is feasible and it would enhance their potential if the emissive metallic tag renders additional cytotoxicity. Apart from features such as the optima solubility and stability, for drug administration, or the increased therapeutic potential, for reaching less conventional treatable cancers, selectivity of the drugs remains as one of the main challenges to deliver efficient anticancer medicines. In our opinion, achieving cancer cell selectivity and more specifically reaching the right biological target is crucial. Heterometallic optical theranostic agents can help to understand the biological interplay of the drug, facilitating the information gathering for its optimization. Therefore, constant and rigorous work into the development of heterometallic complexes is mandatory. Eventually, reaching the stage of in vivo monitoring and evaluation of these metal-based theranostic agents would be a great step forward for their clinic translation.

Alternatively, multimodal therapy combining chemotherapy, photodynamic therapy with optical imaging techniques seems achievable with heterometallic probes. The non-conventional heterometallic drugs are taking the lead in this category, but still there is a long way to cover. This appealing area of research will surely lead to new metallodrugs in the future, but for the moment only initial prototypes are developed.

Acknowledgements

The authors thank the AEI (Ministerio de Ciencia Innovación y Universidades) for projects PID2019-104379RB-C21, RTI2018-097836-J-I00, RYC2018-025872 and RED2018-102471-T, and Gobierno de Aragón-Fondo Social Europeo (E07_20R) for financial support. M.R. thanks the Gobierno de Aragón for a predoctoral fellowship.

Keywords: metallodrugs • theranosis • anticancer • bioimaging • heterometallic.

References

[1] a) B. Rosengberg, L. VanCamp, T. Trigas, *Nature* **1965**, *205*, 698-699. b) B. Rosengberg, L. VanCamp, J. E. Trosko, V. H. Mansour, *Nature* **1969**, *222*, 385-386.

[2] T. C. Johnstone, G. Y. Park, S. J. Lippard, *Anticancer Res.* **2014**, *34*, 471-476.

[3] R. Oun, Y. E. Moussa, N. J. Wheate, *Dalton Trans.* **2018**, *47*, 6645-6653.

[4] M. G. Apps, E. H. Y. Choi, N. J. Wheate, *Endocr. Relat. Cancer* **2015**, *22*, 219-233.

[5] a) I. Mármol, J. Quero, M. J. Rodríguez-Yoldi, E. Cerrada, *Cancers* **2019**, *11*, 780-816. b) J. P. C. Coverdale, T. Laroiya-McCarron, I. Romero-Canelón, *Inorganics* **2019**, *7*, 31-46.

[6] S. S. Kelkar, T. M. Reineke, *Bioconjugate Chem.* **2011**, *22*, 1879–1903.

[7] a) A. R. Kherlopian, T. Song, Q. Duan, M. A. Neimark, M. J. Po, J. K. Gohagan, A. F. Laine, *BMC Syst. Biol*. **2008**, *2*, 74-92. b) M. Baker, *Nature* **2010**, 463, 977-979.

[8] a) F. Rost, "Fluorescence microscopy applications" in Encyclopedia of Spectroscopy and Spectrometry **2017**, pp. 627-631. b) C. M. St. Croix, S. H. Shand, S. C. Watkins, *BioTechniques* **2005**, *39*, S2-S5. doi 10.2144/000112089. c) C. A. Combs, *Curr. Protoc. Neurosci.* **2010**, *50*, 2.1.1-2.1.14. DOI: 10.1002/0471142301.ns0201s50.

[9] a) J. Li, Y. Liu, Y. Xu, L. Li, Y. Sun, W. Huang, *Coord. Chem. Rev*. **2020**, *415*, 213318-213330. b) Y. Sun, F. Ding, Z. Chen, R. Zhang, C. Li, Y. Xu, Y. Zhang, R. Ni, X. Li, G. Yang, Y. Sun, P. J. Stang, *PNAS* **2019**, *116*, 16729-16735.

[10] a) Y. Sun, F. Ding, Z. Zhou, C. Li, M. Pu, Y. Xu, Y. Zhan, X. Lu, H. Li, G. Yang, Y. Sun, P. J. Stang, *PNAS* **2019**, *116*, 1968-1973. b) Y. Sun, F. Ding, Z. Chen, R. Zhang, C. Li, Y. Xu, Y. Zhang, R. Ni, X. Li, G. Yang, Y. Sun, P. J. Stang, *PNAS* **2019**, *116*, 16729-16735. c) F. Ding, Z. Chen, W. Y. Kim, A. Sharma, C. Li, Q. Ouyang, H. Zhu, G. Yang, Y. Sun, J. S. Kim, *Chem. Sci*. **2019**, *10*, 7023-7028.

[11] a) J. Shum, P. K.-K. Leung, K. K.-W. Lo, *Inorg. Chem.* **2019**, *58*, 2231-2247. b) C. Caporale, M. Massi, *Coord. Chem. Rev*. **2018**, *363*, 71-91. c) K. Y. Zhang, Q. Yu, H. Wei, S. Liu, Q. Zhao, W. Huang, *Chem. Rev.* **2018**, *118*, 1770-1839. d) K. K.-W. Lo, *Acc. Chem. Res.* **2015**, *48*, 2985-2995. e) V. Fernández-Moreira, M. P. Coogan, *Chem. Commun*. **2014**, *50*, 384-399. f) E. Baggaley, J. A. Weinstein, J. A. G. Williams, *Coord. Chem. Rev*. **2012**, *256*, 1762-1785. g) V. Fernández-Moreira, F. L. Thorp-Greenwood, M. P. Coogan, *Chem. Commun.* **2010**, *46*, 186-202.

[12] a) T. M. Stonelake, K. A. Phillips, H. Y. Otaif, Z. C. Edwardson, P. N. Horton, S. J. Coles, J. M. Beames, S. J. A. Pope, *Inorg. Chem.* **2020**, *59*, 2266−2277. b) C. B. Larsen, H. van der Salm, G. E. Shillito, N. T. Lucas, K. C. Gordon, *Inorg. Chem.* **2016**, *55*, 8446-8458. c) H. Shahroosvand, P. Abbasi, A. Faghih, E. Mohajerani, M. Janghouri, M. Mahmoudi, *RSC Adv*. **2014**, *4*, 1150-1154.

[13] M. Y. Berezin, S. Achilefu, *Chem. Rev.* **2010**, *110*, 2641-2684.

[14] W. Yang, S.-L. Chen, *J. Innov. Opt. Health Sci.* **2020,** *13*, 2030006-2030026.

[15] V. Fernández-Moreira, M. C. Gimeno, *Chem. Eur. J.* **2018**, *24*, 3345-3353.

[16] M. Wenzel, E. Bigaeva, P. Richard, P. Le Gendre, M. Picquet, A. Casini, E. Bodio, *J. Inorg. Biochem.* **2014**, *141*, 10-16.

[17] F. Pelletier, V. Comte, A. Massard, M. Wenzel, S. Toulot, P. Richard, M. Picquet, P. Le Gendre, O. Zava, F. Edafe, A. Casini, P. J. Dyson, *J. Med. Chem.* **2010**, *53*, 6923-6933.

[18] a) F. Pelletier, V. Comte, A. Massard, M. Wenzel, S. Toulot, P. Richard, M. Picquet, P. Le Gendre, O. Zava, F. Edafe, A. Casini, P. J. Dyson, *J. Med. Chem.* **2010**, *53*, 6923-6933. b) H. Goitia, Y. Nieto, M. D. Villacampa, C. Kasper, A. Laguna, M. C. Gimeno, *Organometallics* **2013**, *32*, 6069-6078. c) S. Gençaslan, W. S. Sheldrick, *Eur. J. Inorg. Chem.* **2005**, *19,* 3840–3849. d) L. Massai, J. Fernández-Gallardo, A. Guerri, A. Arcangeli, S. Pillozzi, M. Contel, L. Messori, *DaltonTrans.* **2015**, *44*, 11067-11076. e) A. Johnson, I. Marzo and M. C. Gimeno, *Dalton Trans.* **2020**, *49*, 11736-11742.

[19] M. Milkevitch , B. W. Shirley , K. J. Brewer, *Inorg. Chim. Acta* **1997**, *264*, 249-256. b) K. Sakai, H. Ozawa, H. Yamada, T. Tsubomura, M. Hara, A. Higuchi, M. A. Haga, *Dalton Trans.* **2006**, *27*, 3300-3305.

[20] M. Cusumano, M. L. Di Pietro, A. Giannetto, *Inorg. Chem.* **2006**, *45*, 230-235.

[21] M. G. Karaaslana, A. Aktaşa, C. Gürsesb, Y. Göka, B. Ateş, *Bioor. Chem.* **2020**, *95*, 103552-103566.

[22] V. Fernández-Moreira, I. Marzo, M. C. Gimeno, *Chem. Sci.* **2014**, *5*, 4434-4446.

[23] A. Luengo, V. Fernández-Moreira, I. Marzo, M. C. Gimeno, *Inorg. Chem.* **2017**, *56*, 15159-15170.

[24] A. Luengo, V. Fernández-Moreira, I. Marzo, and M. C. Gimeno, *Organometallics* **2018**, *37*, 3993-4001.

[25] A. Luengo, M. Redrado, I. Marzo, V. Fernández-Moreira, M. C. Gimeno, *Inorg. Chem.* **2020**, *59*, 8960-8970.

[26] L. Boselli, M. Carraz, S. Mazères, L. Paloque, G. González, F. Benoit-Vical, A. Valentin, C. Hemmert, H. Gornitzka, *Organometallics* **2015**, *34*, 1046-1055.

[27] M. Mora, M. C. Gimeno, R. Visbal, *Chem. Soc. Rev.* **2019**, *48*, 447-462.

[28] M. Wenzel, A. de Almeida, E. Bigaeva, P. Kavanagh, M. Picquet, P. Le Gendre, E. Bodio, A. Casini, *Inorg. Chem.* **2016**, *55*, 2544−2557.

[29] P. J. Jarman, F. Noakes, S. Fairbanks, K. Smitten, I. K. Griffiths, H. K. Saeed, J. A. Thomas, C. Smythe. *J. Am. Chem. Soc*. **2019**, *141*, 2925−2937.

[30] a) C. Caporale, C. A. Bader, A. Sorvina, K. D. M. MaGee, B. W. Skelton, T. A Gillam, P. J. Wright, P. Raiteri, S. Satgni, J. L. Morrison, S. E. Plush, D. A. Brooks, M. Massi, *Chem. Eur. J.* **2017**, *23*, 15666-15679.

b) S. Moromizato, Y. Hisamatsu, T. Suzuki, Y. Matsuo, R. Abe, S. Aoki, *Inorg. Chem.* **2012**, *51*, 12697-12706.
[31] A. Zamora, G. Vigueras, V. Rodríguez, M. D. Santana, J. Ruiz, *Coord. Chem. Rev*. **2018**, *360*, 34-76.
[32] S. K. Tripathy, U. De, N. Dehury, S. Pal, H. S. Kim, S. Patra, *Dalton Trans.* **2014**, *43*, 14546-14549.
[33] C. A. Puckett, J. K. Barton, *Biochemistry* **2008**, *47*, 11711-11716.
[34] A. Luengo, I. Marzo M. Reback, I. M. Daubit, V. Fernández-Moreira, N. Metzler-Nolte, M. C. Gimeno, *Chem. Eur.J.* **2020**, *26*,12158 –12167.
[35] a) H.-T. Liu, X.-G. Xiong, P. D. Dau, Y.-L. Wang, D.-L. Huang, J. Li, L.-S. Wang, *Nat Commun.* **2013**, *4*, 2223; Erratum in: *Nat Commun.* **2018**, *9*, 16200. b) I. León, F. Ruipérez, J. M. Ugalde, L.-S. *Wang, J. Chem. Phys.* **2016** ,*145*, 064304.
[36] S. Sun, J. Wang, D. Mu, J. Wang, Y. Bao, B. Qiao, X. Peng, *Chem. Commun.* **2014**, *50*, 9149-9152.
[37] A. Wragg, M. R. Gill, D. Turton, H. Adams, T. M. Roseveare, C. Smythe, X. Su, J. A. Thomas, *Chem. Eur. J.* **2014**, *20*, 14004-14011.
[38] C. Zhang, R. Guan, X. Liao, C. Ouyang, T. W. Rees, J. Liu, Y. Chen, L. Jia, H. Chao, *Chem. Commun.* **2019**, *55*, 12547-12550.
[39] M. G. Walker, P. J. Jarman, M. R. Gill, X. Tian, H. Ahmad, P. A. N. Reddy, L. McKenzie, J. A. Weinstein, A. J. H. M. Meijer, G. Battaglia, C. G. W. Smythe, J. A. Thomas, *Chem. Eur. J.* **2016**, *22*, 5996-6000.
[40] H. K. Saeed, S. Sreedharan, P. J. Jarman, S. A. Archer, S. D. Fairbanks, S. P. Foxon, A. J. Auty, D. Chekulaev, T. Keane, A. J. H. M. Meijer, J. A. Weinstein, C. G. W. Smythe, J. Bernardino de la Serna, J. A. Thomas, *J. Am. Chem. Soc.* **2020**, *142*, 1101-1111.

10.1002/cmdc.202000833

WILEY-VCH

Entry for the Table of Contents

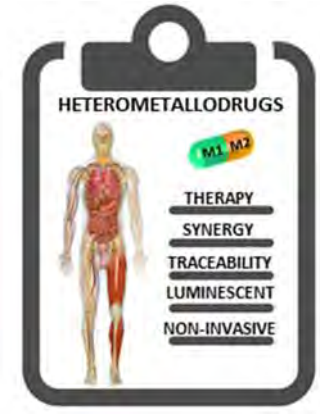

Heterometallic drugs are evolving as a great alternative to conventional drugs. Combination of different metallic fragments enhances therapeutic potential and endows the drugs with traceability, delivering a new class of theranostic agents. The well-stablished therapeutic potential of Pt^{II}, Ru^{II} and Au^{I} based drugs, and d^6 transition metal complexes makes an excellent partnership for the development of novel traceable heterometallodrugs.

Institute and/or researcher Twitter usernames: @GimenoGroup @VanesaFM_ISQCH @ISQCH_Divulga